RESEARCH ACTIVITIES

Isotope Effect on the Fluorescence Cross Section for the Dissociative Exctation Processes. I. CH_3CN and CD_3CN.

A. HIRAYA, S. OHSHIMA*, Y. MATSUMOTO,** K. TABAYASHI, and K. SHOBATAKE
Institute for Molecular Science, Myodaiji, Okazaki, 444 Japan
* Dept. of Chem., Toho Univ., Funabashi, Chiba, 274, Japan
** Inst. of Chem. & Phys. Research, Wako, Saitama, 351, Japan

The relative cross section and quantum yield of fluorescence from the nascent $CN^*(B,A)$ formed by photodissociative excitation of acetonitrile-h_3 and -d_3 were determined in the wave length region of exciting photon between 105 and 150 nm on the fluorescence apparatus for vapor phase photochemistry using UVSOR synchrotron radiation as a light source. Figure 1a and 1b show the absortion and the fluorescence cross section againt the excitation photon wave length for CD_3CN and CH_3CN, respectively. The quantum yield for emission from the excited photofragment $CN^*(B,A)$ formed by the reaction:[1,2]

$$CX_3CN + h\nu \longrightarrow CX_3CN^{**}$$
$$\longrightarrow CX_3 + CN^*(B,A) \quad (X = H, D)$$

has been found to increase gradually with photon energy. We have also found that the fluorescence quantum yields for two isotopic compounds are almost identical in the valence band region above 130 nm, while that for the CD_3CN is about a factor of two larger than the one for CH_3CN in the Rydberg transition region below 125 nm. The present findings are explained in light of the isotope effect of competing dissociation channels involving the motion of hydrogen atoms in the methyl group, such as formation of CH_2CN + H, CHCN + H_2, CH_2 + HCN. Preliminary measurements of the fluorescence excitation spectra of HCN and DCN show that the quantum yields for $CN^*(B\longrightarrow X)$ emission from the photofragments are almost identical for two hydrogen isotopic compunds except for some isotopic shifts in vibrational frequencies, which makes a contrast to the findings on the CX_3CN system.

1) H. Okabe and V. H. Dibeler, J. Chem. Phys. 59, 2430 (1973).
2) M. N. R. Ashfold and J. P. Simons, J. Chem. Soc. Faraday II74, 1263 (1978).

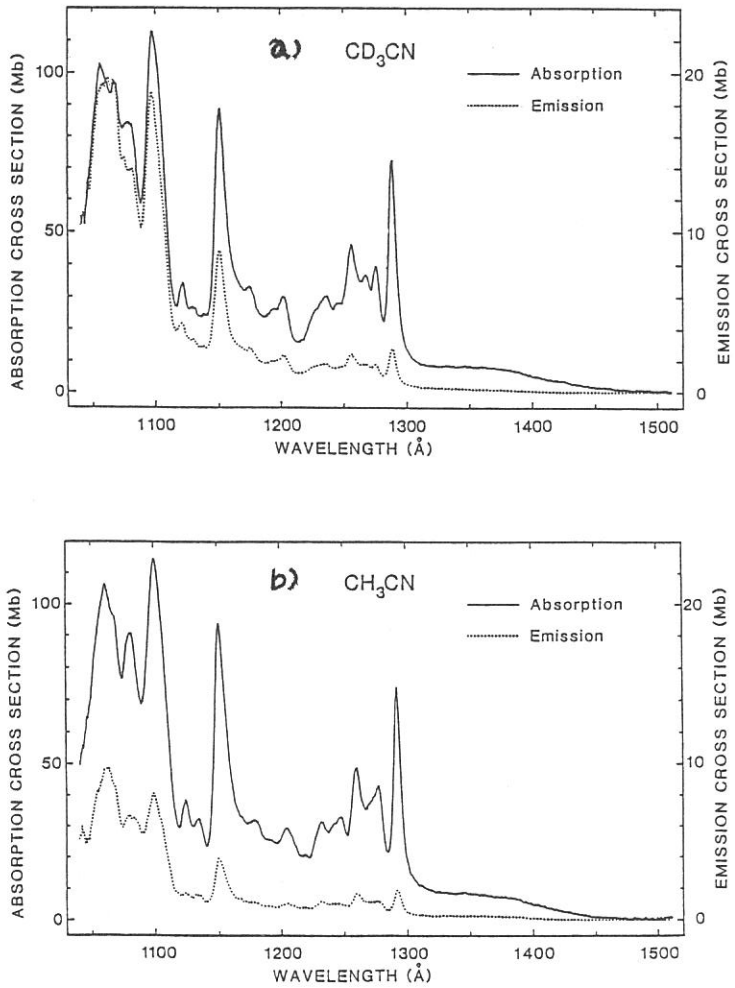

Figure 1. Absorption and fluorescence cross section versus wave length of the exciting photons for CD_3CN (upper) and CH_3CN (lower) in the gas phase. The fluorescence cross section was put on an absolute scale by scaling the fluorescence intensity to that of H_2O whose absolute fluorescence cross section is determined by Lee et al. (J. Phys. B 11,47 (1978)). The resolution of the dispersed synchrotron light was about 5.0 Å.

FLUORESCENCE FROM ION-PAIR AND RYDBERG STATES OF I_2

R.J. DONOVAN*, B.V. O'GRADY*,
Kosuke SHOBATAKE and Atsunari HIRAYA

*Department of Chemistry, University of Edinburgh,
West Mains Road, Edinburgh EH9 3JJ, U.K.
Institute for Molecular Science, Myodaiji, Okazaki 444, Japan.

Absorption and emission excitation spectra of I_2 vapor have been recorded in the wavelength region 105-210 nm using synchrotron radiation from UVSOR. Transparent light intensity was measured by a combination of a sodium salicylate coated window and a photomultiplier. The absorption cross section was determined from the attenuation of light intensity in a cell with an optical path length of 10.9 cm. Fluorescence was viewed at right angle to the incident light and observed at wavelengths longer than the air cut-off (ca. 180 nm).

The measured absorption cross section as a function of wavelength, in the region 105-210 nm, is shown in figure 1. Three broadly different regions in the absorption spectrum are distinguished: the broad feature between 173-205 nm is due to ion-pair absorption assigned as $D(0_u^+) \leftarrow X(0_g^+)$[1], and the sharp bands between 132-176 nm are due mainly to Rydberg transitions, and the broad continuous absorption is due to photoionization.

As shown in figure 1, the strongest fluorescence band is observed in the region 173-205 nm associated with the $D(0_u^+)$ ion-pair state. It is striking that fluorescence is not observed from the C_6 Rydberg system (175 nm)[2]. Because of low sensitivity of the fluorescence measurement system in this wavelength region, it can not be said whether C_6 Rydberg state fluoresce or not. But, it was strongly suggested[3] that there is a fast dissociation channel from C_6 Rydberg system.

An interesting feature of this band is the structure observed 175-182 nm, composed of several dips. The location of the first member of these dips in 173-178 nm coincides with those of the strong C_6 Rydberg absorption system. From the appearance of these dips in the fluorescence band associated with the $D(0_u^+)$ ion-pair state, it is concluded that this ion-

pair state is strongly mixed with sparse vibrational levels of non-fluorescent C_6 Rydberg state. Another strong fluorescence dip is observed at 182nm. Although no assignment is attempted here for the state which is responsible for this dip, it would appear that the $D(0_u^+)$ ion-pair state is strongly perturbed in this region and is probably predissociated.

Intense fluorescence is again observed for shorter wavelength than 151 nm. From the dispersed fluorescence spectra[3], it is found that the excitation to the C_7 Rydberg system (150 nm) gives rise to the emission from an ion-pair state. This is another evidence for perturbation between the Rydberg and ion-pair states. Below 149 nm, predissociation can yield electronically excited iodine atom. Actually, emission from both 6s $^4P_{5/2}$ and 6s $^2P_{3/2}$ states of atomic iodine have been observed[3].

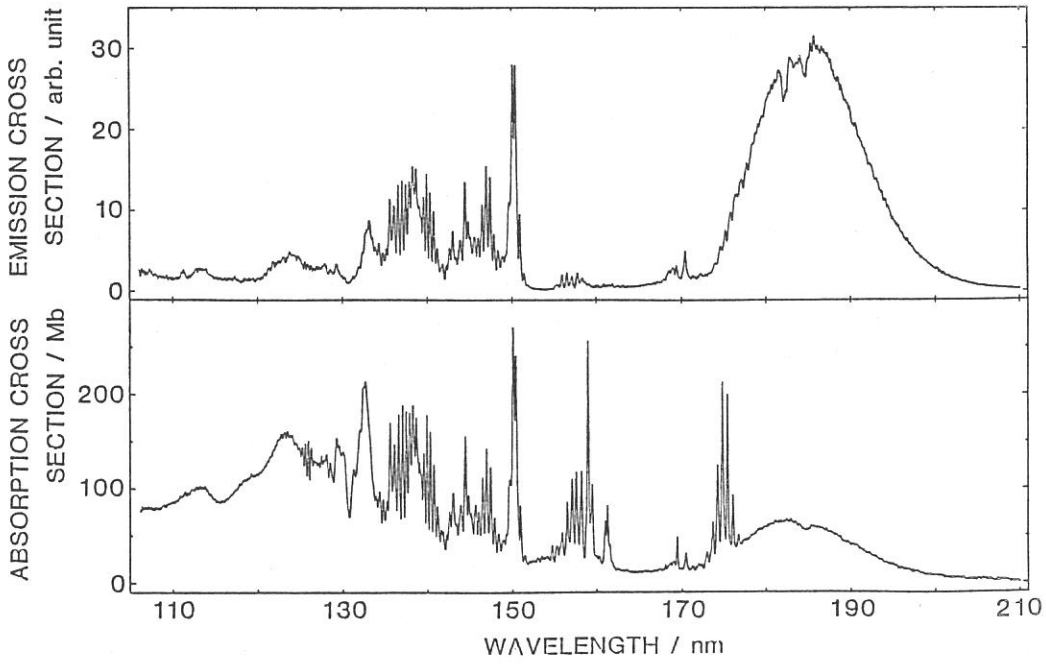

Fig. 1. Absorption (lower) and fluorescence excitation (upper) spectra of I_2 vapor (11 mtorr).

1. R.S. Mulliken, J.Chem.Phys., 55, 288 (1971)
2. P. Venkateswarlu, Can. J.Phys., 48 1055 (1970)
3. Emission spectra of I_2 excited in Rydberg region, next paper.

EMISSION SPECTRA OF I_2 EXCITED IN RYDBERG REGION

Atsunari HIRAYA, Kosuke SHOBATAKE and R.J. DONOVAN*

Institute for Molecular Science, Myodaiji, Okazaki 444, Japan
*Department of Chemistry, University of Edinburgh,
West Mains Road, Edinburgh EH9 3JJ, U.K.

From the fluorescence excitation spectrum of I_2 vapor (105-210 nm) obtained by monitoring longer wavelengths than ca. 180 nm, it was suggested that some emitting states other than optically prepared state are formed following the excitation to the Rydberg systems higher than the C_7 Rydberg system. In an attempt to identify such emitting states, emission spectra of I_2 vapor have been measured in the region above 180 nm.

The emission spectrum excited at the peak position (150 nm) of the C_7 Rydberg absorption system is shown in figure 1(a). The strongest emission band is observed at 183 nm. Following this band at longer wavelength region weak continuous emission band system with maxima at 216, 236, and 270 nm is observed. Further weak bands are also observed at 304, 323, and 340 nm. In the emission spectrum excited at 137 nm, where several Rydberg absorption systems are overlapped, is shown in figure 1(b). Two strong emission bands at 183 and 206 nm, and very weak bands at 323 and 340 nm are observed. The general feature of the emission spectra excited in the Rydberg systems higher than the C_7 Rydberg system is the same as that excited at 137 nm. In these emission bands, two emission bands at 323 and 340 nm appear more prominently under higher pressure conditions. These two emission bands can be assigned as the D → X (323nm)[1] and D' → A' (340nm)[2] ion-pair

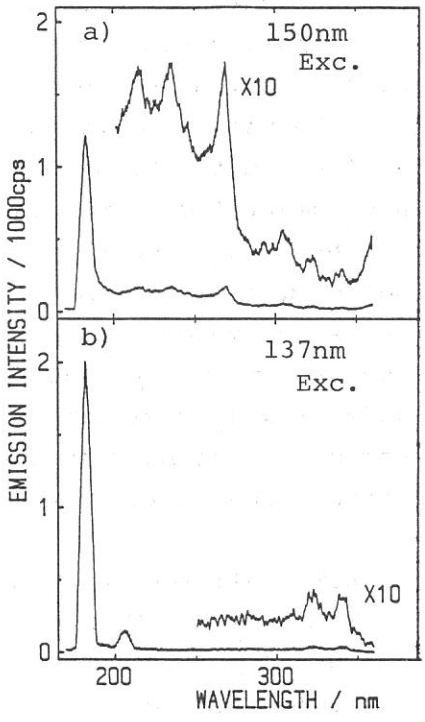

Figure. 1. Emission spectra of I_2

emission bands in which the emitting states are formed by collisions.

On the other hand, five emission bands located at shorter wavelength than 310 nm are not affected by the sample gas pressure. Two of these primary emission bands, 183 and 206 nm, can be assigned as the 6s $^4P_{5/2} \rightarrow 5p^5\ ^2P_{3/2}$ and 6s $^2P_{3/2} \rightarrow 5p^5\ ^2P_{1/2}$ transitions of iodine atom, respectively. From the excitation spectra monitored at both 183 and 206 nm emission, the onset for the formation of 6s $^4P_{5/2}$ and that of 6s $^2P_{3/2}$ states were found to lie at 150 ± 0.5 nm and 146 ± 1 nm, respectively.

The 270 nm band was observed in the emission spectrum under high pressure conditions, and assigned as the emission from the F ion-pair state[3] formed by collisions to the ground state of I_2. It should be noted that the 270 nm band observed here, following the excitation to the C_7 Rydberg system, is not the collision induced emission band. And it has been suggested from the absorption spectrum that the C_7 Rydberg system is quite strongly perturbed[4]. From these observations, it is concluded that the C_7 Rydberg system is strongly mixed with the F ion-pair state and thus the excitation to the C_7 Rydberg state results in the emission from F ion-pair state.

So far the emitting states produced following the excitation to the Rydberg states under low pressure condition are identified as two excited states of iodine atom (6s $P_{5/2}$ and 6s $^2P_{3/2}$) and the F ion-pair state. When Xe is added as a buffer gas, emission from XeI^* excimer become dominant irrespective of excitation wavelengths shorter than 192 nm, except for the C_6 Rydberg state which does not fluoresce even under low I_2 pressure without Xe. From these results, it is strongly suggested that a very fast dissociation to the ground state atoms takes place from the C_6 Rydberg state.

1. R.S. Mulliken, J.Chem.Phys., 55, 288 (1971).
2. K.P. Lawley, M.A. MacDonald, R.J. Donovan and Agust Kvaran, Chem.Phys.Lett., 92, 322 (1982).
3. H.Hemmati and G.J. Collins, Chem.Phys.Lett., 75, 488 (1980)
4. R.J. Donovan, B.V.O'grady, K.Shobatake and A.Hiraya, Chem.Phys.Lett., 122, 612 (1985).

$CCl_2(\tilde{A}^1B_1)$ RADICAL FORMATION IN THE VUV PHOTOLYSES OF CCl_4 AND $CBrCl_3$

Toshio IBUKI, Atsunari HIRAYA* and Kosuke SHOBATAKE*

Institute for Chemical Reserach, Kyoto University, Uji, Kyoto 611
*Institute for Molecular Science, Myodaiji, Okazaki 444

Gas-phase CCl_2 radical has been generated in various ways. Laser induced fluorescence(LIF) bands have been detected in the 500-560 nm range[1] and band structures have been partially resolved.[2] The LIF method also has shown that the radiative lifetime of the electronically excited $\tilde{A}^1B_1$ state is 3.81 ± 0.30 μsec.[3] In the present work $CCl_2(\tilde{A}^1B_1)$ radical is formed by the direct photodecomposition of CCl_4 and $CBrCl_3$ molecules using Lyman-α or Ar I resonance lines. The absorption and fluorescence excitation spectra of CCl_4 and $CBrCl_3$ are measured on a fluorescence apparatus at the BL-2A station of UVSOR.

Fig. 1 shows the emission observed when CCl_4 was photolyzed by a H Lyman-α lamp. Quite similar spectrum devoid of structure was found in the case of $CBrCl_3$ photoexcitation. The time dependence of the fluorescence decay was found to be expressed by a superposition of two lifetime components of 1.9 and 3.2 μsec at the extrapolated zero pressure by using a pulser which emits about 10 nsec(FWHM) light of 121.6 nm.

The observed emission was assigned as the $CCl_2(\tilde{A}^1B_1 \rightarrow \tilde{X}^1A_1)$ transition based on the following observations:

(1) Absorption bands of CCl_2 ($\tilde{A} \leftarrow \tilde{X}$) transition appear in the 440-560 nm range,[4] which overlaps with the present emission wavelength region.

(2) The spectral feature in Fig. 1 resembles well to the chemiluminescence spectrum(diffuse band in the 400-800 nm range) observed in a Ba + CCl_4 reaction,[5] in which the emitter has been assigned as $CCl_2(\tilde{A}^1B_1)$ radical.

(3) The long lifetime component of 3.2 μsec is close to the value of 3.8 μsec in Ref. 3.

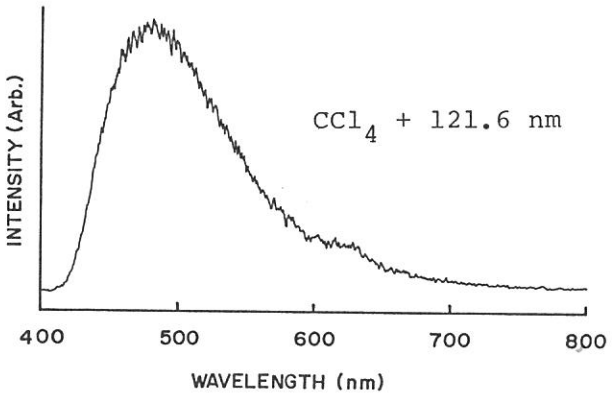

Fig. 1. Dispersed fluorescence.

Absorption and fluorescence excitation spectra of CCl_4 and $CBrCl_3$ are shown in Figs. 2 and 3, respectively. Although quite weak fluorescence can be observed at the beginning of the first excited states of CCl_4 and $CBrCl_3$, sharp increases of emission intensities at around 143 nm(8.7 eV) in Figs. 2 and 3 indicate the following decomposition processes:

$$CCl_4 + h\nu \rightarrow CCl_2(\tilde{A}^1B_1) + 2Cl \qquad \Delta H \simeq 8.9 \text{ eV}$$

$$CBrCl_3 + h\nu \rightarrow CCl_2(\tilde{A}^1B_1) + Br + Cl \qquad \Delta H \simeq 8.3 \text{ eV}$$

where ΔH values were calculated by the observation that the emissions are found at $\lambda > 405$ nm.

Assignments of the absorption peaks of CCl_4 have been given by Causley and Russell.[6] However, we have found no previous study on the quantitative absorption spectrum of $CBrCl_3$ in the VUV range. The valence configuration of $CBrCl_3$ is $(3a_1)^2(4e)^4(1a_2)^2(5e)^4$.[7] We tentatively assign the Rydberg bands in Fig. 3 as follows:

nm	Transition
185.0	$5e \rightarrow \sigma^*$
157.5	$5e \rightarrow ns(3/2)$
152.0	$5e \rightarrow ns(1/2)$
145.5	$4e \rightarrow ns$
136.7	$5e \rightarrow np(3/2)$
134.7	$1a_2 \rightarrow np$
133.0	$5e \rightarrow np(1/2)$
130.0	$4e \rightarrow np$
115.5	$3a_1 \rightarrow np$
113.5	$(5e)^{-1}$ (3/2)
111.0	$(5e)^{-1}$ (1/2)

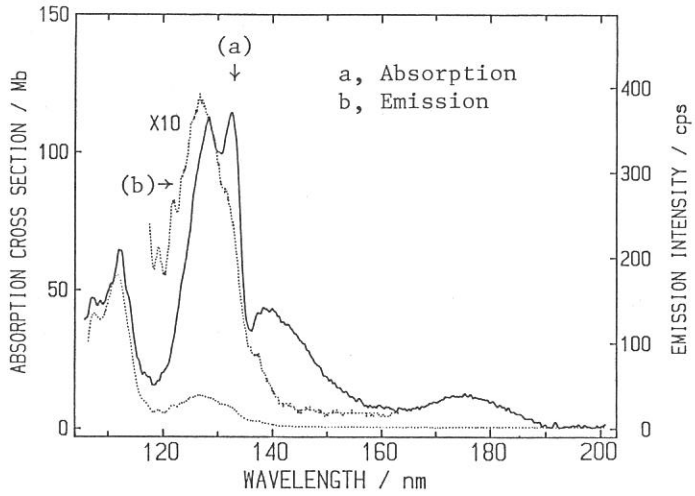

Fig. 2. Absorption and fluorescence excitation spectra of CCl_4.

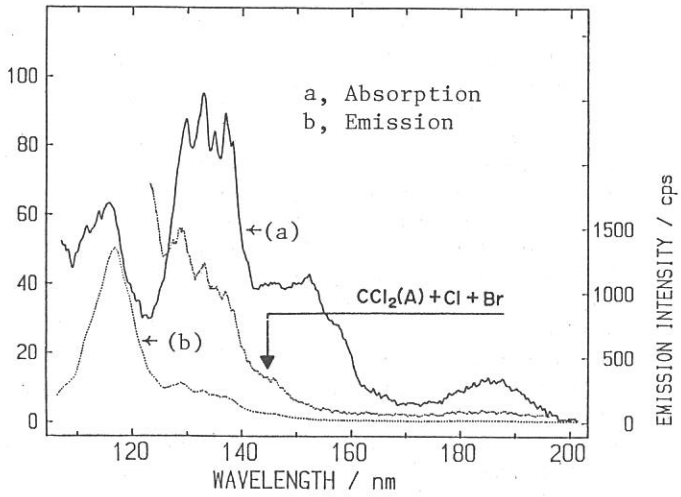

Fig. 3. Absorption and fluorescence excitation spectra of $CBrCl_3$.

References

1) J. J. Tiee, F. B. Wampler and W. W. Price, Chem. Phys. Lett., 65, 425 (1979).
2) D. A. Predmore, A. M. Murray and M. D. Harmony, Chem. Phys. Lett., 110, 173 (1984).
3) R. E. Huie, N. J. T. Long and B. A. Thrush, Chem. Phys. Lett., 51, 197 (1977).
4) D. E. Milligan and M. E. Jacox, J. Chem. Phys., 47, 703 (1967).
5) R. Kiefer, A. Siegel and A. Schultz, Chem. Phys. Lett., 59, 298 (1977).
6) G. C. Causley and B. R. Russell, J. Electron Spectrosc. Relat. Phenom., 11, 383 (1977).
7) I. Novak, T. Cvitas and L. Klamsinc, J. Chem. Soc., Faraday Trans. 2, 77, 2049 (1981).

ABSORPTION AND FLUORESCENCE SPECTRA OF CH_3SCN AND RELATED MOLECULES

Ikuo TOKUE, Atsunari HIRAYA*, and Kosuke SHOBATAKE*

Department of Chemistry, Niigata University, Niigata 950-21
*Institute for Molecular Science, Myodaiji, Okazaki 444

Vacuum UV photolysis of CH_3SCN and CH_3NCS produces fluorescence attributed to SCN(A, B) radicals[1]. The emission spectra of the CH_3S radicals is obtained in the photolysis of $(CH_3)_2S$[2]. In this study, the photoabsorption and fluorescence cross sections of CH_3SCN, CH_3NCS, CH_3NCO, and $(CH_3)_2S$ were measured in the 105-210 nm region and the emission spectra from the excited fragments were observed in the 300-500 nm region.

Synchrotron radiation dispersed by a 1 m Seya-Namioka monochromator was used as the light source. The dispersed photon flux entered the gas cell (10.9 cm long) through LiF window. The photon flux was measured by using a combination of sodium salicylate coated LiF window and a photomultiplier. The total fluorescence in the 160-650 nm region was observed at right angle to the primary photon beam. The emission from the excited photofragments dispersed by a Nikon P250 monochromator was observed in the 300-500 nm region. The sample vapor was continuously introduced into the gas cell and slowly pumped by a rotary pump. All chemicals were degassed at 77 K.

In the absorption of CH_3NCS, several valence-type transitions are very intense, while no Rydberg progression is observed. On the other hand, for CH_3SCN, CH_3NCO, and $(CH_3)_2S$, a number of absorption were found to fit Rydberg progressions of the form, $\nu_n = IP - R/(n-\delta)^2$, where IP and R are the ionization potential and the Rydberg constant, respectively. In all three spectra, the initial member of each series is assigned an n of 4, which restricts δ (the quantum defect) to 1-2. Three Rydberg series constructed for each molecule are, according to convention, the s, p, and d Rydberg series, respectively. The values of δ and IP are listed in Table 1. The values for $(CH_3)_2S$ are in good agreement with those in the literature[3]. The absorption and fluorescence cross sections(c.s.) of CH_3SCN are shown in Fig. 1 with three Rydberg progressions indicated. The fluorescence c.s. shows structure corresponding to the absorption c.s.

The emission spectra observed from excitation of CH_3SCN at 152.6 ± 1 and 125.6 ± 1 nm are shown in Fig. 2. The emission spectrum obtained at 152.6 nm is assigned to the SCN(A-X) and SCN(B-X) bands, while that obtained at 125.6 nm is mainly attributed to the CN(B-X) band. The photodissociation pro-

cesses that produce these excited photofragments are

$$CH_3 \begin{cases} \rightarrow CH_3(X^2A_2'') + SCN(A^2\Pi/B^2\Sigma^+), & \Delta H=6.39/6.49 \text{ eV}, \quad (1) \\ \rightarrow CH_3S(X^2E) + CN(B^2\Sigma^+), & \Delta H=7.45 \text{ eV}, \quad (2) \end{cases}$$

where the ΔH values represent the enthalpy of dissociation. The threshold wavelength for Reaction 2 is $\approx$166 nm. The CN(B) species seems to have a little contribution to the fluorescence produced at 152.6 nm.

The emission spectrum observed from excitation of CH_3NCS at 153.5±1 nm is identical with that from CH_3SCN at 152.6 nm excitation and is assigned to the NCS band. The emission spectra observed from CH_3NCO (λ_{exc}=138±1 nm) and $(CH_3)_2S$ (λ_{exc}=152±1 nm) are assigned to the NCO(A-X) and CH_3S(A-X) bands, respectively.

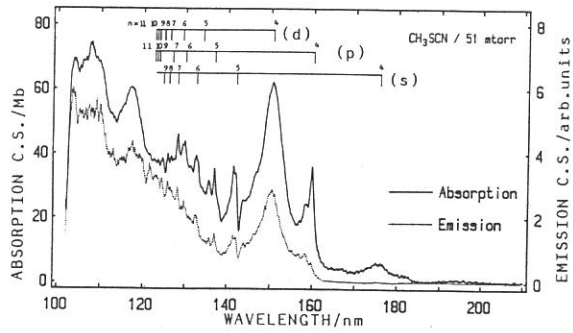

Fig. 1. The absorption and total fluorescence c.s. of CH_3SCN

Table I IP and δ of CH_3SCN, CH_3NCO, and $(CH_3)_2S$

Molecule	series	δ	IP/cm^{-1}
CH_3SCN	s (n=4-10)	1.92	80727
	p (n=4-11)	1.58	81071
	d (n=4-11)	1.20	80995
CH_3NCO	s (n=4-11)	1.98	86050
	p (n=4-11)	1.58	86030
	d (n=4-10)	1.23	86217
$(CH_3)_2S$	s (n=4-12)	2.00	70006
	p (n=4-11)	1.60	70236
	d (n=4-11)	1.19	70073

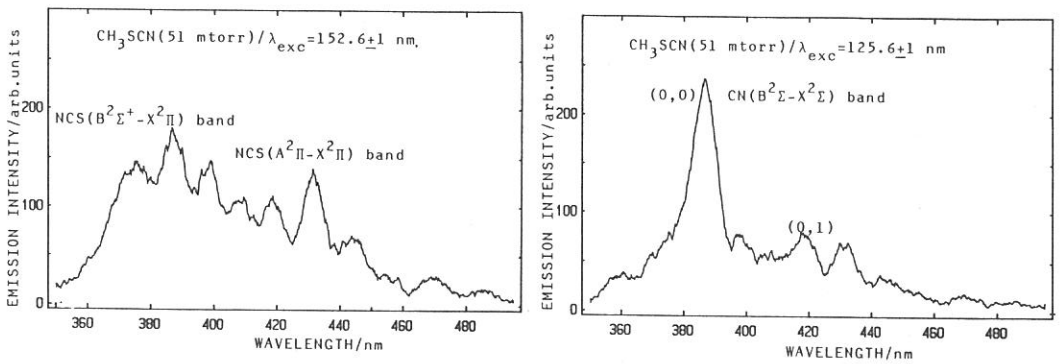

Fig. 2. Emission spectra produced from CH_3SCN at 152.6 nm and 125.6 nm excitation

References: [1] P.D'amario et al., JCS Faraday Trans.I, 68(1972)940. [2] K.Ohbayashi et al., Chem. Phys. Lett., 52(1977)47. [3] J.D.Scott et al., J. Chem. Phys., 59(1973)6577; R. McDiarmid, J. Chem. Phys., 61(1974)274.

DIRECT VUV ABSORPTION MEASUREMENTS OF SUPERSONIC COOLED MOLECULES AND MOLECULAR CLUSTERS

Yohji ACHIBA, Haruo SHIROMARU, and Katsumi KIMURA
Institute for Molecular Science, Myodaiji, Okazaki 444

Investigations of excited state structure and dynamics of molecules are often hindered by limited spectroscopic information available concerning their higher electronic states. Thermal inhomogeneous broadening effects, including sequence band congestion and the overlap of vibronic band rotational envelope, combined with rapid photochemical and photophysical relaxation channels, frequently result in diffuse gas phase absorption spectra displacing little or no vibrational structure.

The technique of supersonic cooling provides a means of producing rotationally and vibrationally cold molecules in the gas phase. Furthermore, recent experimental results have definitely shown that this method is quite useful for producing a large amount of molecular clusters under a collision-free condition.

In this project we have constructed an experimental setup for direct VUV absorption measurements of jet-cooled molecules and molecular clusters. A synchrotron radiation at UVSOR is used as an VUV light source by a 1-m seya monochromator (see also the description on the BL2B2 in the previous section). A gaseous sample is expanded through a pulsed supersonic nozzle ,and then introduced through a skimmer into a photon-melecule interaction region. The SR light is crossed with the supersonic beam, and then detected by a photomultiplier operated at the pulsed frequency. Absorption measurements are performed by operating two pulse counters in our microcomputer system. One of the counters is synchronized with an open phase of the pulsed nozzle, and the other one with closed phase. Such a situation is shown in Figure 1 as a timing chart of the counters. The light intensities of I and I_0 are measured by counters A and B, respectively.

A preliminary experimental result obtained by the present

system is shown in Figure 2. A transmission curve shown in this figure is attributed to the Rydberg series converging to the third ionic state of N_2.

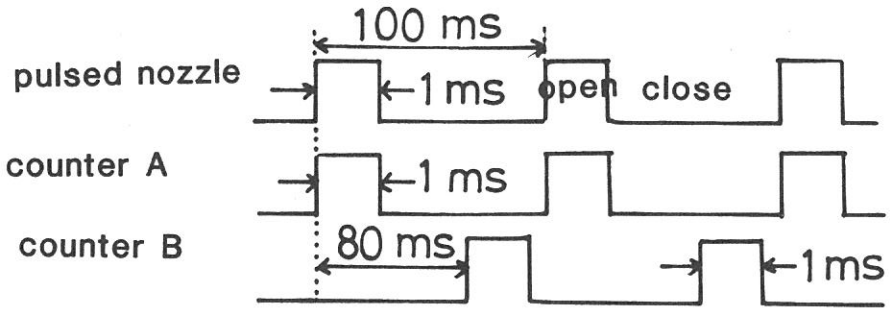

Figure 1 A timing chart of counters A and B as well as a pulsed nozzle.

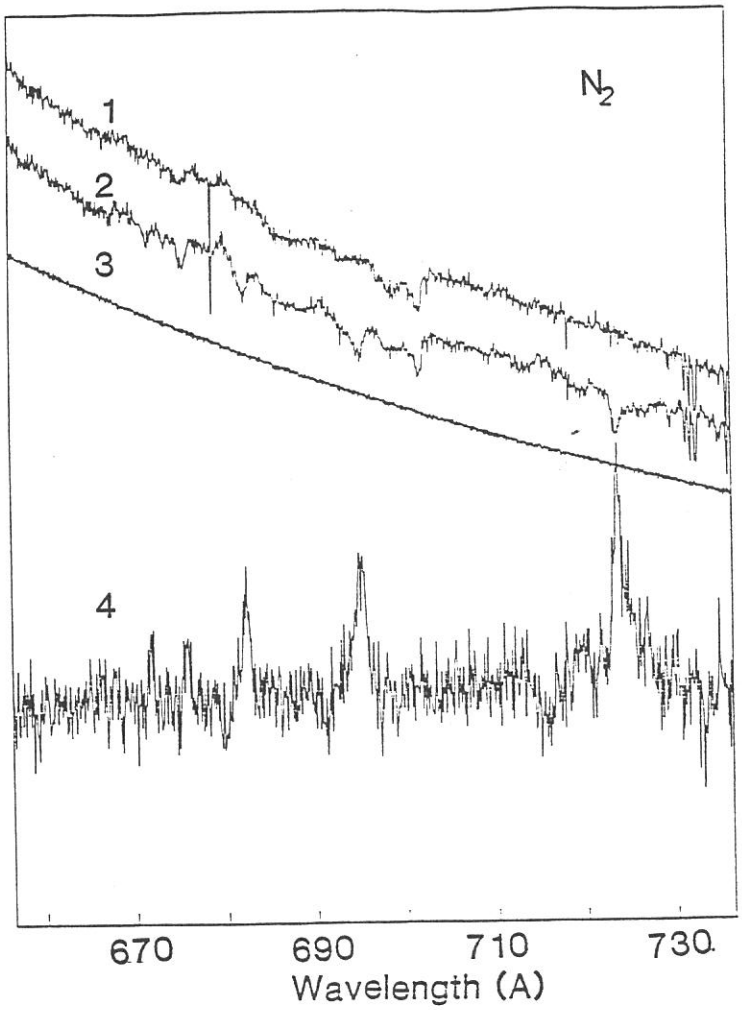

Figure 2

Light intensity curves and a transmission curve of N_2 molecule: Curves 1 and 2 indicate light intensity changes as a function of SR wavelength, where the curve 1 (I_0) is obtained by a counter B, and the curve 2 (I) by a counter B. Curve 3 means an intensity change of an electron beam current. Curve 4 indicates a transmission curve obtained by dividing the curve 2 by the curve 1.

PHOTOIONIZATION OF METHANOL CLUSTERS

Nobuaki WASHIDA*, Yohji ACHIBA, Haruo SHIROMARU, and Katsumi KIMURA

Institute for Molecular Science, Myodaiji, Okazaki 444
*Division of Atmospheric Environment, National Institute for Environmental Studies, Tsukuba-gakuen, Ibaraki 305

The ion molecule reactions of CD_3OH are known to produce ions of $(CD_3OH)H^+$ and $(CD_3OH)D^+$:

$$CD_3OH^+ + CD_3OH \rightarrow (CD_3OH)H^+ + CD_3O \qquad (1a)$$

$$\rightarrow (CD_3OH)D^+ + CD_2OH \qquad (1b)$$

In the present study, Reactions (1a) and (1b) were studied by photoionization of neutral CD_3OH dimer. Fig.1b represents the mass spectrum of CD_3OH clusters photoionized by an Ar resonance lamp (11.83 and 11.62 eV). Signals at m/e=35 and 36 from $(CD_3OH)H^+$ and $(CD_3OH)D^+$, respectively, were observed. Fig.2 summarizes the results of a reduced intensity, $(CD_3OH)_{n-1}D^+/(CD_3OH)_{n-1}H^+$, distributions relative to the cluster size n. In the case of the dimer, the ratio of (1a)/(1b) is 1.2. A question of interest is that the $(CD_3OH)D^+$ is produced from a familiar hydrogen bonded dimer of CD_3OH (A) or another type of dimer (B).

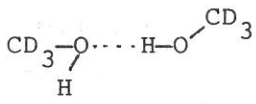

(A)

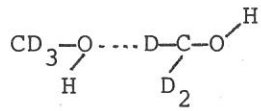

(B)

In order to get an answer, the appearance potentials of $(CD_3OH)H^+$ and $(CD_3OH)D^+$ were measured by using synchrotron orbital radiation. Results are shown in Figs 3 and 4. No significant difference was observed in the photoionization efficiency curves for the $(CD_3OH)H^+$ and $(CD_3OH)D^+$ ions. The results suggest that the precursory dimer of the $(CD_3OH)D^+$ ion is the same as that of the $(CD_3OH)H^+$, probably type A. The deuterium migration may occur in the dimer (A) after ionization.

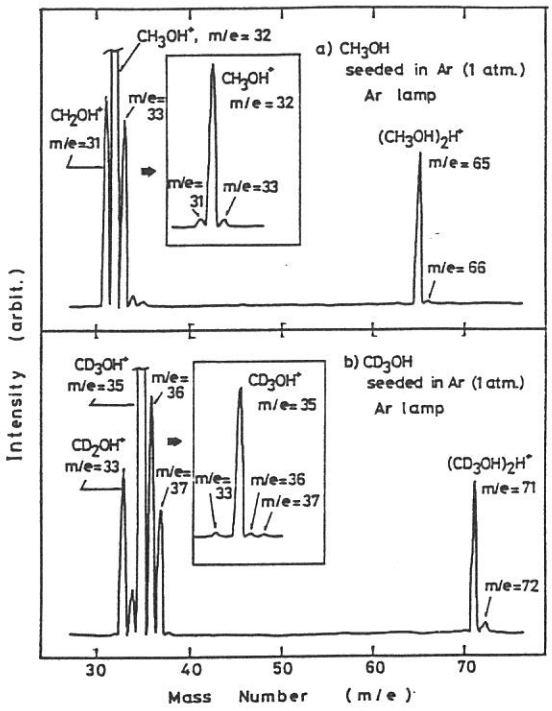

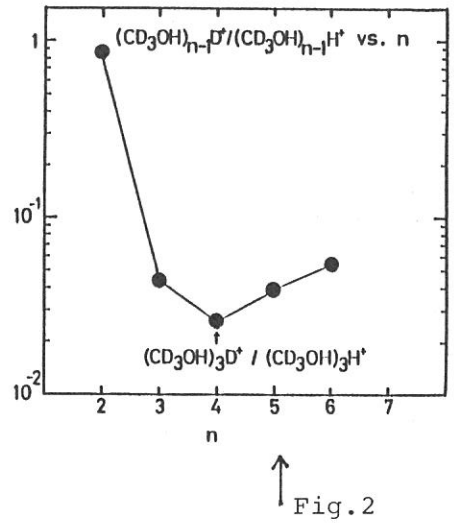

Fig.2

Fig.1

Fig.3

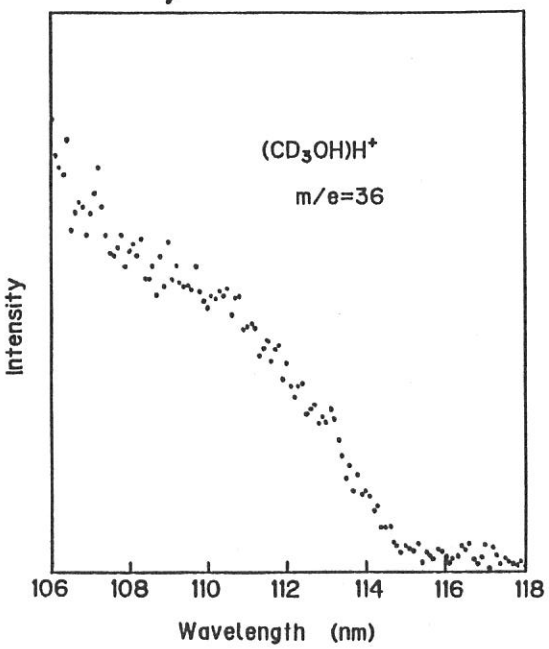

Fig.4

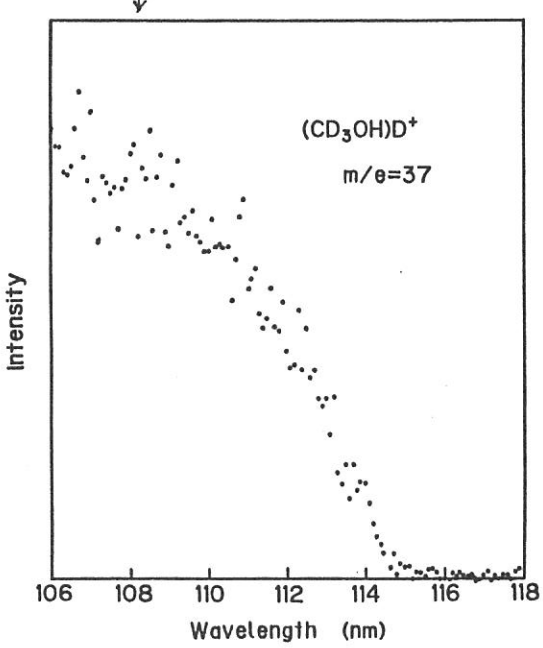

THRESHOLD ELECTRON SPECTRUM AND PHOTOIONIZATION EFFICIENCY CURVE OF CH_3Cl

Shinzo SUZUKI and Inosuke KOYANO

Institute for Molecular Science, Myodaiji, Okazaki 444

Using the TEPSICO-II apparatus described elsewhere,[1,2] we have investigated the threshold electron spectrum (TES) and photoionization efficiency curve (PIEC) of CH_3Cl over the wavelength range from 40 to 120 nm. The ultimate goal here is the state- or internal energy-selected studies of unimolecular and bimolecular processes of molecular ions, utilizing a coincidence measurements of various ions with threshold electrons.

Figure 1 shows the threshold electron spectrum of CH_3Cl taken with the incident photon resolution of about 0.02 nm. Four major bands are clearly seen; the complex first band which is assigned to the ^2E ground state of the ion, the broad structureless second and third bands which respectively correspond to the removal of a σa_1 and π_e electron, and the weak fourth band which has not been observed in the He I photoelectron spectra because of its energy. Compared with the He I spectra,[3] the second and third bands are seen to be relatively much stronger in the TES.

Ions observed in the wavelength range studied are parent ion CH_3Cl^+ and two fragment ions CH_3^+ and CH_2Cl^+. In Fig. 2 we present an ionization efficiency curve for the CH_3^+ fragment. The weak broad peak above 900 nm

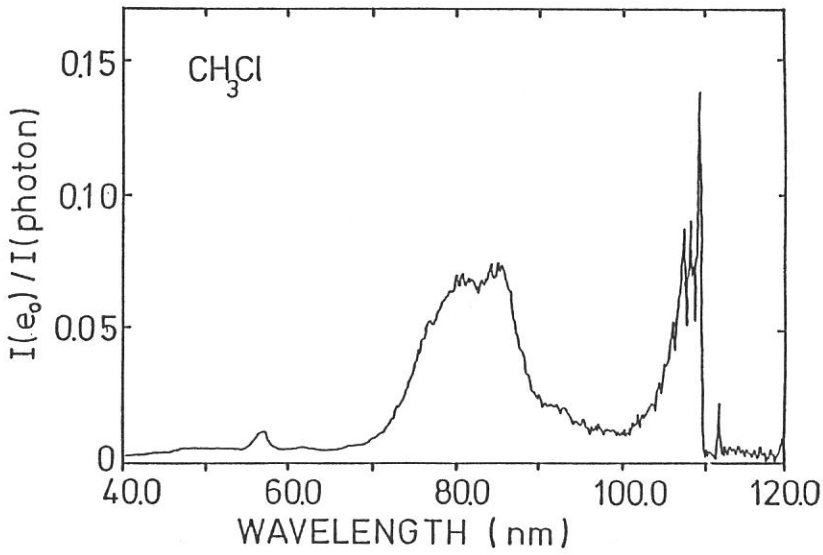

Fig. 1 Threshold electron spectrum of CH_3Cl

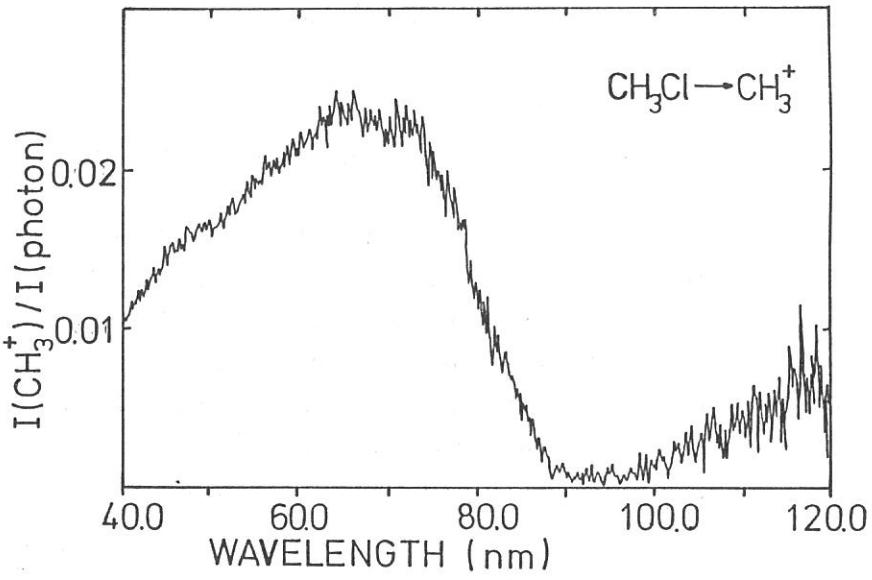

Fig. 2 Photoionization efficiency curve for CH_3^+ from CH_3Cl

corresponds to the ion - pair process $CH_3Cl + h\nu \rightarrow CH_3^+ + Cl^-$, whose cross section decreases monotonically toward the first ionization onset of the molecule. No rise in the CH_3^+ efficiency is seen at the ionization onset nor at any wavelength in the range corresponding to the formation of the ground state ions, indicating that ions in this state are nondissociative. The second huge peak in the PIEC starts to rise at about 90 nm , the wavelength that exactly coincides with the onset of the second band in the TES, and keeps rising throughout the region of the second and third TES bands, until it reaches a maximum at 65 - 70 nm where no threshold electrons are observed. All these facts indicate that CH_3^+ is produced through excitation to the second and/or third electronic state(s) of the parent ion and that this excitation is most efficiently accomplished by photons of somewhat shorter wavelengths than the thresholds. It is not certain, on the other hand, whether the fourth state is dissociated to give CH_3^+ or not. The coincidence experiments with these threshold electrons would shed light to these problems.

References

1 I. Koyano, K. Tanaka, T. Kato, and E. Ishiguro, in this Report.
2 I. Koyano, K. Tanaka, T. Kato, S. Suzuki, and E. Ishiguro, Nucl. Instr. Meth., in print (1986).
3 D. W. Turner, C. Baker, A. D. Baker,and C. R. Brundle, Molecular Photoelectron Spectroscopy (Wiley - Interscience, New York, 1970); K. Kimura, S. Katsumata, Y. Achiba, T. Yamazaki, and S. Iwata, Handbook of He I Photoelectron Spectra of Fundamental Organic Molecules (Japan Scientific Society, Tokyo, 1981).

INVESTIGATION OF DEEP VALENCE AND CORE LEVEL EXCITATION IN VOLATILE COMPOUNDS WITH GROUP IV ELEMENTS USING UVSOR

Shin-ichi NAGAOKA, Shinzo SUZUKI and Inosuke KOYANO

Institute for Molecular Science, Myodaiji, Okazaki 444

Shallow valence level excitation and the subsequent fragmentation of many molecules have been studied extensively using several kinds of light sources in recent years. However, the processes following deep valence and core level excitation have not been investigated in detail so far, because, for the purposes of such investigations, the conventional light sources are insufficient in both photon energy and intensity. The synchrotron radiation is expected to provide a powerful means to obtain information about the deep level excitation. Volatile compounds with group IV elements are particularly suitable for detailed investigations of the above-mentioned processes in the vapor phase, because the rather small binding energies of the d core levels allow the studies in the normal incidence region. Accordingly, we have initiated the studies of the deep valence and core level excitation and the subsequent fragmentation in such compounds, using UVSOR. Here, we report preliminary observations of threshold electron spectra of $Sn(CH_3)_4$ and $GeCl_4$ in the wavelength range between 30 and 65 nm.

The experiments were performed using the TEPSICO-II apparatus at BL3B, which has a 3m normal incidence monochromator. The threshold electron spectra were obtained by dividing the threshold electron intensity by that of the exciting light. Experimental results are shown in Fig. 1.

In Fig. 1 the solid line represents the threshold electron spectrum of $Sn(CH_3)_4$, which was taken with the slit width of 0.2 mm. The bands located at 40.0 and 42.4 nm (31.0 and 29.2 eV, respectively) are assigned to the $4d_{3/2}$ and $4d_{5/2}$ core levels, respectively. The 4d core binding energy obtained is in good agreement with that estimated by X-ray

photoelectron spectroscopy (30.4 eV).[1] The band at 58.7 nm (21.1 eV) is considered to be related to the a_1 and/or t_2 molecular orbital(s).

In Fig. 1 the dotted line represents the threshold electron spectrum of $GeCl_4$, which was taken with the slit width of 0.3 mm. The band located at 33.9 nm (36.6 eV) is tentatively assigned to the $3d_{5/2}$ core level. Since the photon intensity of the monochromatized light is weak in the wavelength range below 35 nm, we cannot determine the 3d core binding energy unambiguously. The bands at 51.9 and 59.8 nm (23.9 and 20.7 eV, respectively) are considered to be related to the a_1 and t_2 molecular orbital(s), respectively.

Further investigations, including the threshold electron - fragment ion coincidence measurement, are in progress.

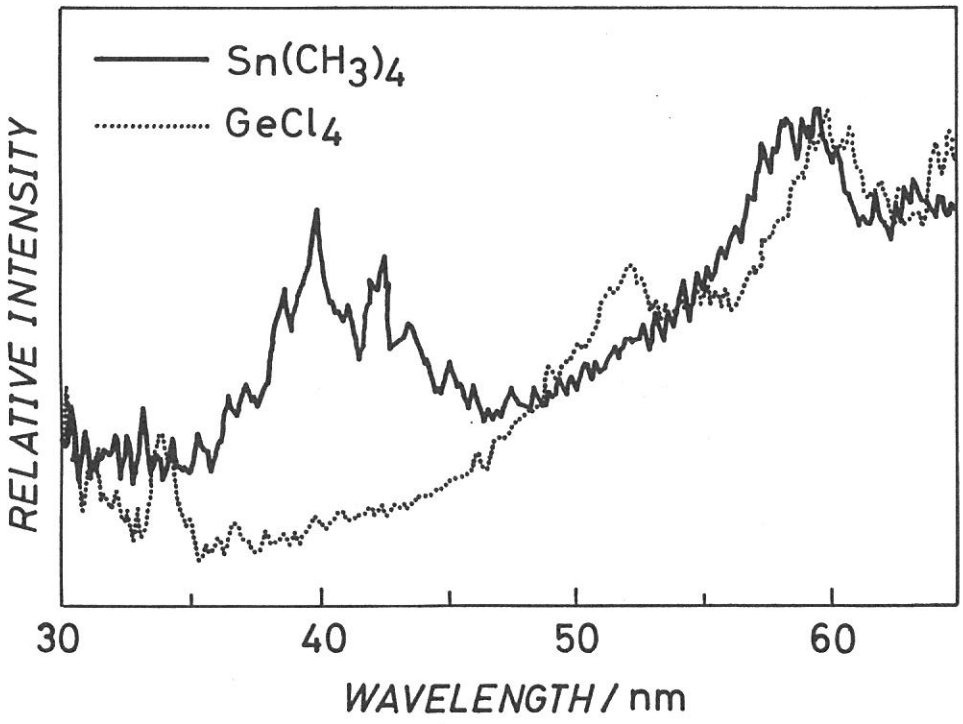

Fig. 1 Threshold electron spectra of $Sn(CH_3)_4$ and $GeCl_4$

Reference

1. S. C. Avanzino and W. L. Jolly, J. Electron Spectrosc. Relat. Phenom., 8 (1976) 15.

Polarized Reflection Spectra of Orthorhombic Indium Bromide in 2 - 100 eV Region

Kaizo NAKAMURA, Yasuo SASAKI, Makoto WATANABE* and Masami FUJITA+

Department of Physics, Kyoto University, Kyoto 606
*Institute for Molecular Science, Okazaki 444
+Maritime Safety Academy, Kure 737

Reflection spectra of orthorhombic indium bromide crystal (InBr: space group D_{2h}^{17}) have been investigated at LHeT by using synchrotron radiation and its polarization characteristics in the energy region between 2 and 100 eV. Single crystal of InBr was grown by Bridgman method which was cleaved into thin slabs with ac-surface. Two platelets of InBr were mounted on the sample holder of cryostat to get polarized reflection spectra. Light from 600 MeV storage ring was monochromatized with the plane grating monochromator (PGM) at BL6A2. Energy range 2 - 100 eV can be covered with five spectral ranges with the combination of two gratings and five mirrors. Vacuum in the sample chamber was kept less than 10^{-9} Torr. Incident and reflected light was detected with a photomultiplier coated with sodium salicylate, which is rotatable around the specimen.

Figure 1(a) shows the spectra for polarization parallel to the c-axis (E//c) and (b) for the a-axis (E//a). They are highly dichroic reflecting the anisotropy of the crystal.

In the low energy region (2 - 4 eV), both spectra are consistent with the previous results.[1] The first exciton peak at 2.33 eV is due to the transition from the top valence band, which consists mainly of In 5s orbital, to In 5p conduction band bottom. This transition is allowed for E//c.

Structure between 3 and 15 eV is classified into 2 groups: One from Br 4p valence band, lying in the lower energy region, and the other from In 5s valence band. Identification of each fine structure rests much upon the development of the band structure

calculation involving the spin-orbit interaction. Above 10 eV intensity begins to diminish.

At about 20 eV sharp doublet structure with the separation of 0.8 eV are observed in both spectra. These are identified as In 4d core exciton (In N_V and N_{IV}).[2] These are also dichroic and composed of 5 components altogether. Possible transitions inferred from the atomic picture of In^+ in the C_{2v} environment cannot explain the dichroic nature clearly. It is necessary to get more detailed information of the covalent character of the In in the TlI crystal structure. At about 75 eV a broad structure is observed resulting possibly from core levels of both In and Br.

References

1) M. Yoshida, N. Ohno, H. Watanabe, K. Nakamura and Y. Nakai: J. Phys. Soc. Jpn 53 (1984) 408.
2) J. A. Bearden and A. F. Burr: Rev. Mod. Phys. 39 (1967) 125.

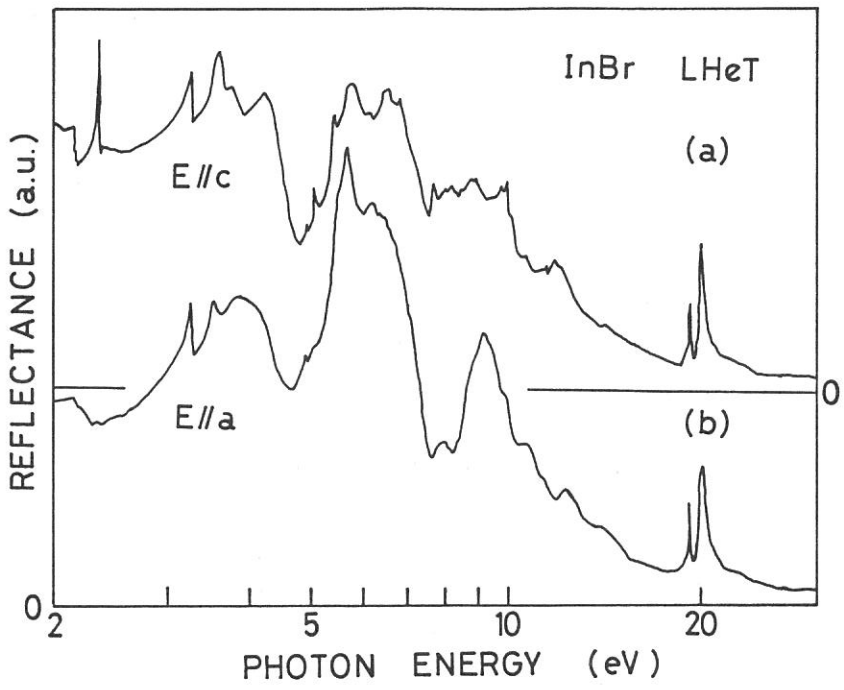

Fig. 1. Reflection spectra of InBr at liquid helium temperature. (a) for E//c and (b) for E//a.

Reflection and Luminescence Excitation Spectra of Cadmium Halide Crystals

Hideyuki NAKAGAWA, Yukio SHIMAMOTO*, Hiroaki MATSUMOTO*, Masami FUJITA**, Takeshi MIYANAGA***, Kazutishi FUKUI and Makoto WATANABE

Institute for Molecular Science, Myodaiji, Okazaki 444
* Department of Electronics, Fukui University, Bunkyo, Fukui 910
** Maritime Safety Academy, Wakaba, Kure 737
*** Department of Physics, Faculty of Education, Wakayama University, Sakaedani, Wakayama 640

Reflection and luminescence excitation spectra in cadmium bromide and iodide crystals were measured at 5 K and 78 K using synchrotron radiation from SOR-RING of IMS as a light source for the energy range up to 100 eV. The SR was monochromatized with a plane grating monochromator and was incident on the crystal nearly along the crystal c-axis.

Two groups of well resolved structures are observed at 5 K in the reflection spectra below 10 eV as shown in Fig. 1. These structures are almost the same as those previously reported by Kondo et al.(1) and by Lemonnier et al.(2). They are interpreted as due to the excitonic transitions associated with those from the upper valence band of halogen p-like character to the lowest conduction band of cadmium s-like character. Structures in the low and the high energy groups are connected to the excitonic transitions at the Γ point and at the Z ($CdBr_2$) or A (CdI_2) point in the BZ, respectively.

In the higher energy region from 10 to 15 eV appear several less pronounced structures, the origins of which are not clear at present. The excitonic and the band-to-band transitions from the halogen s-like states to the higher p-like conduction states may be related to these structures.

Doublet structures are observed clearly at 15.67 and 16.35 eV in $CdBr_2$ and at 15.13 and 15.83 eV in CdI_2 as shown in Fig. 2. These structures are connected to the Cd^{2+} $N_{IV,V}$ core excitonic transitions, that is, the optical excitation from the Cd^{2+} $4d_{5/2}$ and $4d_{3/2}$ states to the upper conduction states of cadmium 5p-like character. The splitting energies of the doublets are 0.68 eV in $CdBr_2$ and 0.70 eV in CdI_2 and are considered to correspond to the $N_{IV,V}$ splitting energy of the cadmium atom, ~1.0 eV. The chemical shift

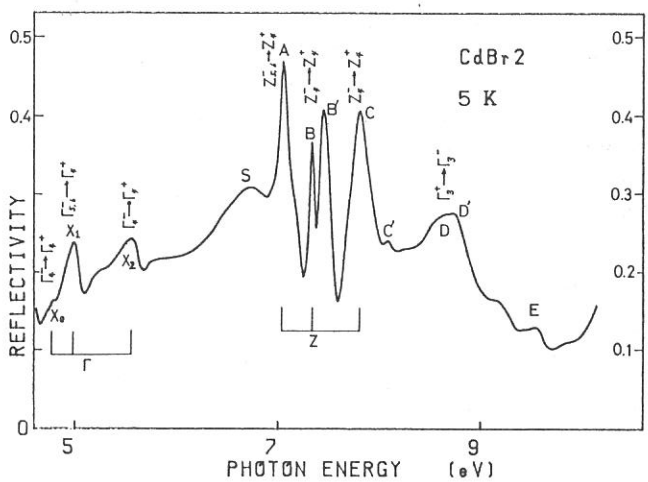

Fig.1 Nearly normal incidence optical reflectivity spectrum of the cleaved surface of $CdBr_2$ single crystals measured at 5 K in the energy region below 10 eV.

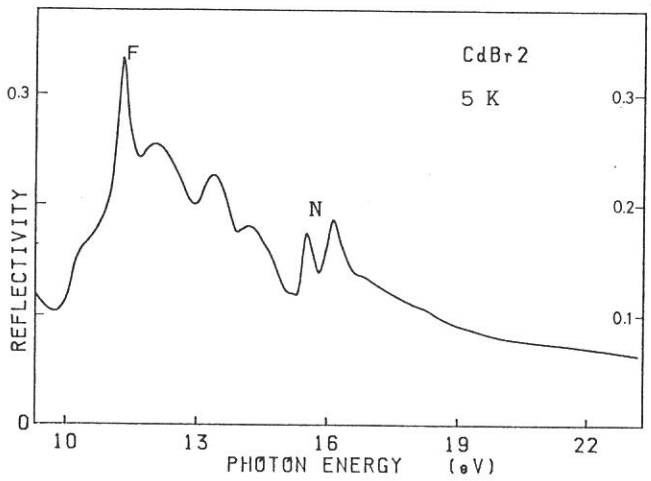

Fig.2 Nearly normal incidence optical reflectivity spectrum of the cleaved surface of $CdBr_2$ single crystals measured at 5 K in the energy region from 10 to 22 eV. The doublet structure indicated by the label N is considered to be due to the cadmium d-core excitons.

of the structures between bromide and iodide are likely to be due to the mixing of the halogen p-orbitals to the upper conduction states. Several substructures are also discernible on and around the doublets. They are attributed to the crystal field splitting arising from the axial symmetry of the cadmium halide crystals. Dichroic measurements will reveal more detailed structures of the core excitons.

It was not possible in the present experiments to resolve reliable structures due to the halogen inner core excitonic transitions which are expected to appear in the energy region from 30 to 100 eV.

Luminescence excitation spectra were measured at 5 K in the direction perpendicular to the crystal c-axis. At this temperature, it is well known that the only one emission band appears in the near ultraviolet region; at 3.30 eV in $CdBr_2$ and at 3.36 eV in CdI_2. In the excitation spectra below 20 eV are observed sharp dips corresponding to the peaks in the reflection spectra. Relative intensity of luminescence is enhanced with increase of the excitation energy in the region from 10 to 20 eV. The first stage of the increase begins at about 9.8 eV which corresponds to the double energy of the lowest excitons. The onset of the second stage is observed as a rapid increase in the intensity at around 13 eV which is over double the energy of the band-to-band gap. The abrupt increase of the luminescence intensity suggests the existence of multiple exciton production processes (3). More quantitative experiments on luminescence yield are nescessary to make further discussions on these processes.

In the higher energy regions up to 100 eV, no clear structures are observed and the luminescence intensity is almost independent of the excitation energy. Irradiation in these regions produces a new emission band at 1.5 eV in the CdI_2 crystal, which may be connected to the defect production caused by the high energy light irradiation.

References

(1) S.Kondo and H.Matsumoto: J.Phys.Soc.Jpn. 51 (1982) 1441.
(2) J.C.Lemonnier, I.Pollini, J.Thomas and A.Lenselink: 7-th International Conference on VUV, p252.
(3) M.Yanagihara, Y.Kondo and H.Kanzaki: J.Phys.Soc.Jpn. 52 (1983) 4397.

RARE-EARTH $N_{4,5}$ ABSORPTION SPECTRA OF SOME RARE-EARTH COMPOUNDS

Kenjiro TSUTSUMI, Osamu AITA, Kouichi ICHIKAWA,
Masao KAMADA, and Makoto OKUSAWA

College of Engineering, University of Osaka Prefecture,
Mozu, Sakai, Osaka 591

The electronic property of rare-earth compounds and alloys containing a partially filled 4f shell has been a subject of theoretical and experimental studies because the rare-earth ions in some of these substances are in a homogeneous mixed-valence state. Among these substances SmB_6 is known to be a typical example, and the investigation of mixed-valence system of this substance has been performed by many experimental methods such as x-ray photoelectron spectroscopy (XPS)[1] and Sm L absorption spectroscopy.[2]

In the $N_{4,5}$ absorption spectra of rare earths sharp structures appear near the threshold. These structures are interpreted as originating from the electronic transition of the 4d electron to the localized unoccupied 4f level. Because of a strong exchange interaction between the $4f^{n+1}$ electrons and the 4d hole, the resultant multiplet levels of the $4d^9 4f^{n+1}$ configuration spread over several tens of electron volts. The purpose of the present study is to investigate whether the Sm $N_{4,5}$ absorption spectrum of a mixed-valence compound SmB_6 represents the multiplet structures originating from the Sm^{2+} and Sm^{3+} ions or not. Also, the $N_{4,5}$ absorption spectra of rare-earth compounds, LaB_6, $LaCl_3$, $CeCl_3$, $SmCl_3$, $EuCl_3$, and $GdCl_3$, were measured for references.

A grazing incidence vacuum spectrometer equipped with a concave grating with the radius of 2 m and the grooves of 1200/mm was used for the measurement. The synchrotron radiation from the storage ring at the Institute for Molecular Science was used as a light source.

Fine structures of the Sm $N_{4,5}$ absorption spectrum of a mixed-valence compound SmB_6 are shown in the figure together with those of $SmCl_3$ which is

believed to be a trivalent substance. The constant-initial-state(CIS) spectra measured by Allen et al.[3] with the initial states at the $4f^6(Sm^{2+})$ and $4f^5(Sm^{3+})$ peaks in the valence band of SmB_6 are also shown by dotted lines. These CIS spectra are believed to represent the 4d photoabsorption structures of the Sm^{2+} and Sm^{3+} ions. The arrows show the 4d ionization thresholds of the Sm^{2+} and Sm^{3+} ions determined by XPS data. As seen from this figure the gross features of the Sm $N_{4,5}$ absorption spectra of SmB_6 and $SmCl_3$ and the CIS spectrum for the Sm^{3+} ion are quite similar one another. This fact suggests that the absorption spectrum of SmB_6 is dominantly attributed to the 4d excitation of the Sm^{3+} ion.

In the case of Sm^{2+} ion the $4d^9 4f^7$ final state caused by the 4d photoabsorption is clearly above the 4d threshold of the Sm^{2+} ion as seen from the CIS spectrum for the Sm^{2+} ion. Therefore, since the final state of the absorption process in the Sm^{2+} ion might involve the $4d^9 4f^n$+(unbound electron in the continuum) state, the structure due to the $4d^9 4f^{n+1}$ excited state is buried in the broad background and this prevents the spectrum from appearing as distinct peaks. While, the CIS spectrum provides the structure only due to the decay, $4d^9 4f^{n+1} \rightarrow 4d^{10} 4f^{n-1}$ + (ejected electron), among the various final states caused by the photoabsorption, and thus the structure due to the Sm^{2+} ion is clearly seen in the CIS spectrum.

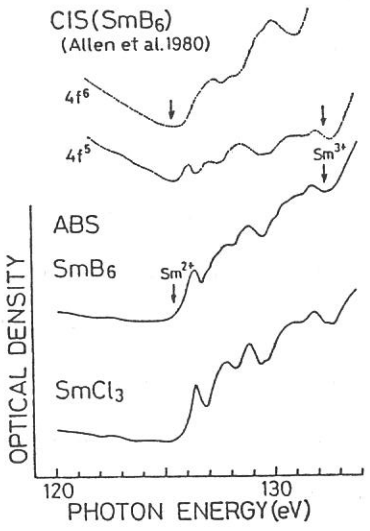

Fig. Fine structures of the Sm $N_{4,5}$ absorption spectra of SmB_6 and $SmCl_3$ and the CIS spectra of SmB_6. Arrows show the 4d ionization thresholds of the Sm^{2+} and Sm^{3+} ions.

References

1) J. -N. Chazalviel, M. Campagna, G. K. Wertheim, and P. H. Schmidt: Phys. Rev. B 14, 4586(1978).
2) M. Okusawa, Y. Iwasaki, K. Tsutsumi, M. Aono, and S. Kawai: Jpn. J. Appl. Phys. 17, Suppl. 17-2, 161(1978).
3) J. W. Allen, L. I. Johansson, I. Lindau, and S. B. Hagstrom: Phys. Rev. B 21, 1335(1980).

Time-Resolved Fluorescence Spectroscopy of Molecular Exciton in Anthracene Single Crystals

Tadaoki MITANI, Takaya YAMANAKA and Iwao YAMAZAKI

Institute for Molecular Science, Myodaiji, Okazaki 444, Japan

Synchrotron radiation from storage ring has a number of advantages as a light source for time-resolved fluorescence and excitation spectroscopies. A high repetition rate of the pulsed time structure enables us to measure a precise subnanosecond time decay by using a time-correlated single-photon counting system. By using an improved 1 m Seya-Namioka type monochromator (see the BI-7B report), we have constructed a computer-aided spectrophotometer available for time-dependent fluorescence and excitation measurements in an energy region of 2-40 eV. The block diagram of this apparatus is shown in Fig. 1. The application of this system to the spectral analysis of fluorescence in anthracene single crystals have been successfully made.

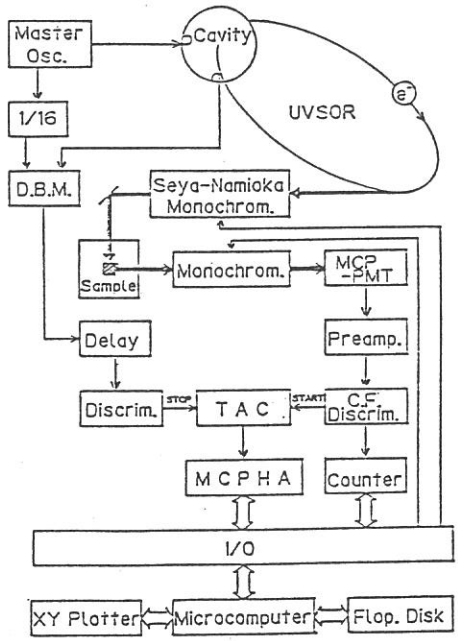

Fig. 1

The time decay of the fluorescence of the singlet exciton in anthracene single crystals exhibits a characteristic dependence on wavelength of the excited light pulse as shown in Fig. 2. For an excitation at a relatively long wavelength, the time decay follows a single-exponential function in more than 3 orders. The life time of the singlet exciton is definitly determined to be 8.6 nsec at 77 K, which is agreement with the previous data. Whereas, by scanning excitation photons to much shorter wavelength, the time decay is remarkably changed and its profile can not be expressed by a single-exponential curve. In addition, the rise time of the emission becomes much faster than the time resolution of the instruments (< 100 psec). Such a characteristic feature of the time decay is clearly reflected in the time-resolved fluorescence spectra in a short time-domain of a few nanosecond as presented in Fig. 3. The spectra of the prompt emission observed within about 300 psec have a simple structure having a tail in a lower energy side. As time going on, the spectrum has more clearly vibrational structures. Then the pectra after about 100 psec are almost independent on time and closely resemble the stationary fluorescence. Thus, the radiative process of the prompt emission is considered to be essentially

different from thcse of the delayed fluorescence in a thermally equilibrium. This implies the presence of an additional radiative-decay channel fcr the higher energy excitations above the threshcld energy of about twice of the excitcn energy.

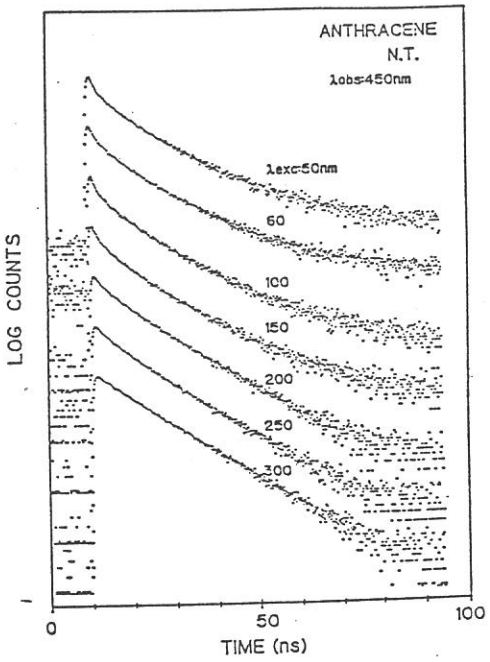

Fig. 2 The time decays of the flucrescence of anthracene crystals at 77 K as a function of excitation wavelength.

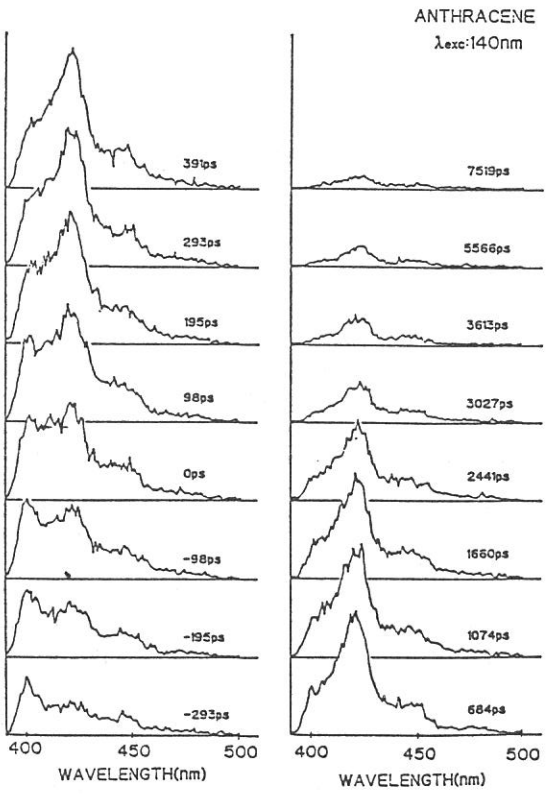

Fig. 3 The time-resclved fluorescence spectra of anthracene crystal at 77 K.

MEASUREMENT OF THE FLUORESCENCE DECAY CURVE USING UVSOR LIGHT PULSE

Tadashi OKADA, Kiyoharu NAKATANI, and Tadaoki MITANI*

Department of Chemistry, Faculty of Engineering Science,
Osaka University, Toyonaka 560
*Institute for Molecular Science, Myodaiji, Okazaki 444

One of the target of interest in photochemical primary processes in condensed phase is to know the dynamical behavior and the relaxation pathways of highly excited molecules in solution which is also studied in the field of radiation chemistry as well as multiphoton laser chemistry.

For the developments of the time resolved detection system using synchrotron radiation in the UV and VUV region, the fluorescence lifetime of the standard compounds were measured by using a time correlated single photon counting electronics coupled with a micro-channel-plate photomultiplier as a detector. Measurements were carried out under the condition of multi-bunch operation of storage ring. An example of the decay curve is illustrated in Figure 1. The time resolution obtained using this system is about 100 ps and has been limited by the walk of timing.

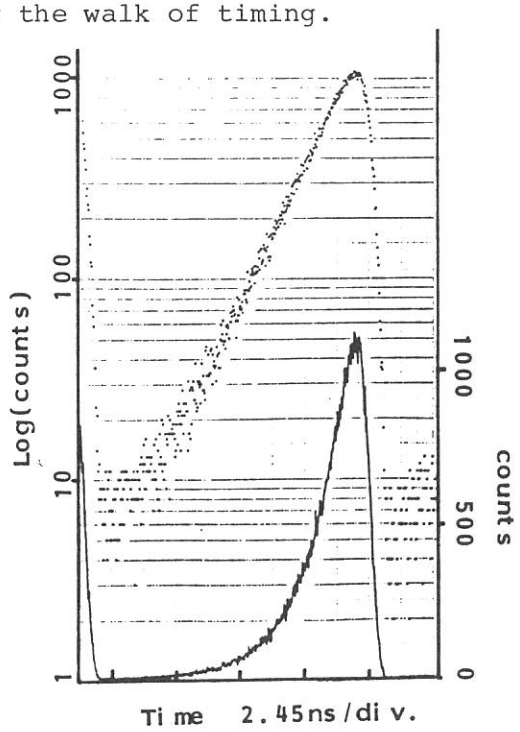

Figure 1. Decay curve of Rhodamine B in aqueous solution. The obtained lifetime was 1.56 ns without deconvolution.

As an application of time resolved spectroscopy to the study of the photoinduced intramolecular electron transfer process in fixed donor-acceptor system, the temperature dependence of the fluorescence decay curve of 4-(N,N-dimethyl aminophenyl)$(CH_2)_2$(9-anthryl) (A_2) in cellulose acetate film has been measured (Figure 2). The results are compared with those obtained by using a streak camera under excitation with picosecond laser pulse.

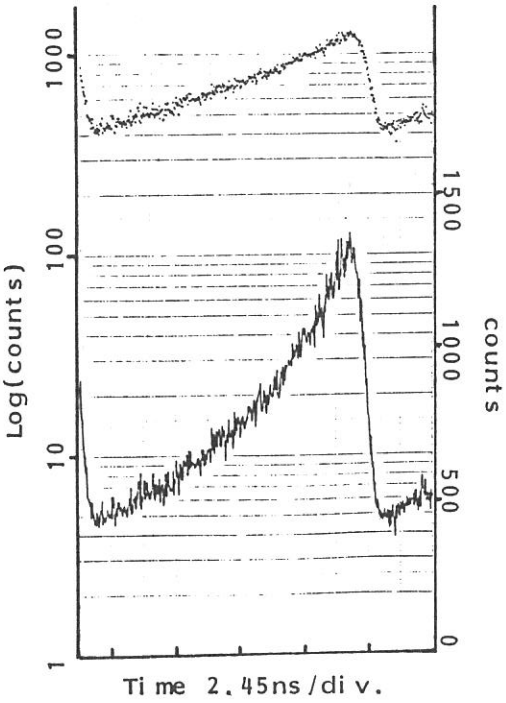

Figure 2. Non-exponential decay curve of the fluorescence of anthracene part of A_2 in cellulose acetate film at 300K.

MEASUREMENTS OF TIME BEHAVIOR OF TRYPTOPHYL FLUORESCENCE BY TIME-CORRELATED SINGLE-PHOTON COUNTING

Atusi KURITA, Shuichi KINOSHITA, Takashi KUSHIDA,
Yuji GOTO, Kozo HAMAGUCHI, and Tadaoki MITANI*

Faculty of Science, Osaka University, Toyonaka 560
* Institute for Molecular Science, Okazaki 444

The combination of highly sensitive single-photon counting and synchrotron radiation pulses having short duration, stable intensity and high repetition rate is considered to be very suitable for the UV spectroscopy with high time resolution and high precision. In order to confirm this, we performed measurements of the decay characteristics of tryptophyl fluorescence by combining UVSOR with our time-correlated single-photon counting system. It is known to be possible with this system to determine a fluorescence decay time as short as several picoseconds by using a CW mode-locked laser as the exciting source.

First, the time profile of the synchrotron radiation pulse was determined. The pulse duration was found to be about 400 ps, which is much narrower than that reported for the Stanford positron-electron accelerator ring of 650 ps. Next, we measured the time behavior of tryptophyl fluorescence around 340 nm in N acetyl-L-tryptophanamide and the constant (C_L) fragments of the immunoglobulin light chain. It was found that the fluorescence intensity shows a single exponential decay in the former, while it has two decay components in the type λ fragment (Figs.1 and 2). The fluorescence time behavior did not change appreciably in both materials, when the excitation wavelength was varied between 220 and 300 nm. The time characteristics of fluorescence depolarization was also obtained successfully.

The constant fragment of immunoglobulin is an interesting material, because it shows no great conformational change on reduction of the only intrachain disulfide bond, which is buried in the interior hydrophobic region. As shown in Fig.3, the fluorescence decay time was found to be lengthened by the reduction of the type λ fragment. This fragment contains two tryptophan residues: one locating close to the disulfide bond, and the other near or on the surface of the protein molecule. On the other hand, the intact type κ fragment, which has only one

tryptophan residue deep inside the molecule, is almost nonfluorescent. When the disulfide bond is reduced, it fluoresces, and its time behavior was found to be very similar to that of the reduced type λ fragment (Fig.4). These results are well explained by the removal of the fluorescence quenching effect of the energy-accepting intrachain disulfide bond.

Although the detailed analysis has not been made yet, the comparison of the time characteristics of the fluorescence anisotropy between the intact and reduced fragments will give valuable information on the internal rotational motions within these macromolecules. Besides the knowledge on the time behavior of tryptophyl fluorescence in proteins, the present experiment demonstrated various advatages of the fluorescence spectroscopy by the combination of UVSOR and the time-correlated single-photon counting technique, such as the high sensitivity, high time resolution, high precision, promptness of the measurement, and tunability of the exciting wavelength.

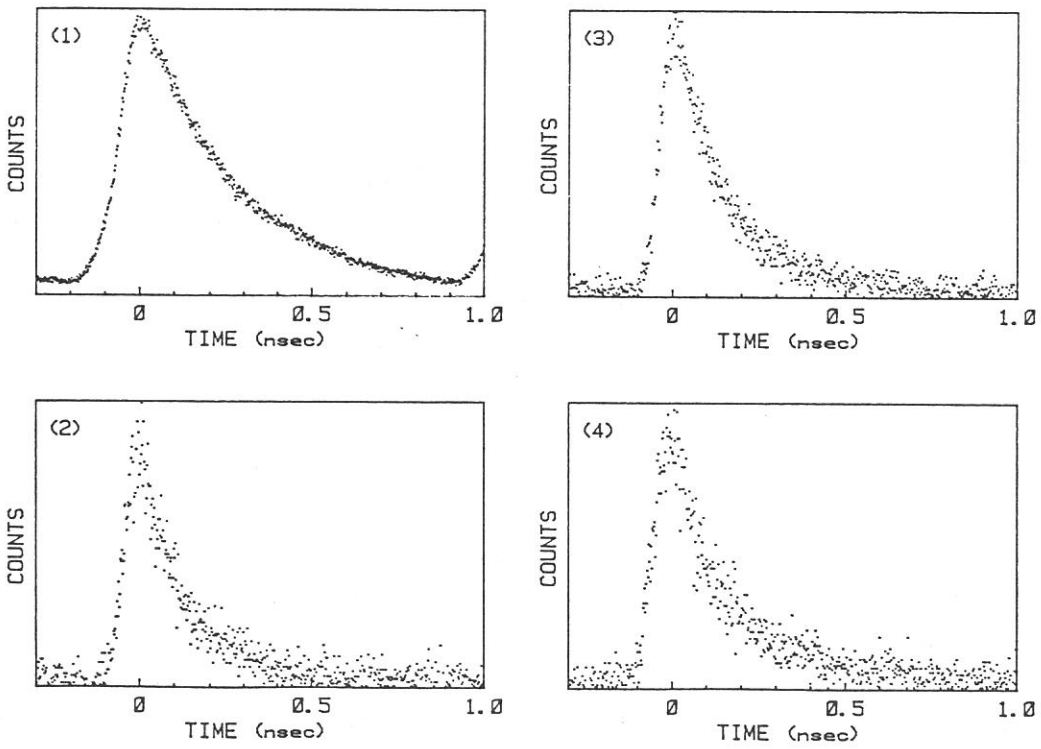

Time behavior of tryptophyl fluorescence of (1) N acetyl-L-tryptophanamide, (2) intact type λ C_L fragment, (3) reduced type λ fragment, and (4) reduced type κ fragment.

PHOTON STIMULATED DESORPTION OF POSITIVE IONS FROM LIF

Tsuneo YASUE, Tetsuji GOTOH*, Ayahiko ICHIMIYA, Yoichi KAWAGUCHI*, Masahiro KOTANI*, Shunsuke OHTANI*, Yukichi SHIGETA*, Shoji TAKAGI*, Yuji TAZAWA* and Goroh TOMINAGA*

Department of Applied Physics, Nagoya University, Nagoya 464
*Institute of Plasma Physics, Nagoya University, Nagoya 464

Resently several observations of photon stimulated desorption (PSD) from alkali halides have been carried out[1-3]. In this paper, we report on the measurements of positive ion yields from LiF as a function of the incident photon energy (the ion yield spectrum), and discuss the mechanism of PSD from LiF.

The experiments were carried out on BL8B2 of UVSOR. LiF (100) surface was cleaved in the air, and the specimen was mounted in a UHV chamber. The sample was heated to about 150 °C to avoid electronic charging during the measurements. The relative photon intensity was measured by the photoelectron ejection from Au. The relative ion yield was normalized with the relative photon intensity.

Figures 1(a) and 1(b) show the relative ion yield spectra of Li^+ and F^+ ions. In Fig. 1(a) there is a rapid rise of ion yield at about 56 eV, and is a weak peak at 58.4 eV. The ion yield increases above 59 eV, and is almost constant up to 67 eV. The spectrum of F^+ ions is similar to that of Li^+ ions below 60 eV. However the considerable difference in the yield spectra is observed above 60 eV. There are a sharp peak at 60.2 eV and a deep valley at 63.5 eV in the F^+ yield spectrum.

In order to consider the mechanism of PSD from LiF, we compare the yield spectra with the photoabsorption spectrum[4]. The rapid rise at about 56 eV and the structure at 58.4 eV is also seen in the photoabsorption spectrum. Those structures are ascribed the core excitation of $Li^+(1s)$ state. Then following two different interatomic transitions are considered;

$$Li^{+*} + F^- \longrightarrow Li^{0*} + F^+ + e^- \qquad (1)$$

and

$$Li^{+*} + F^{-} \longrightarrow Li^{+} + F^{0} + e^{-}, \qquad (2)$$

where asterisks indicate the core-excited states. The Madelung constant for the final state of eq. (1) is negative and that of eq. (2) is positive. Therefore the process of eq. (1) is dominant for PSD of positive ions from LiF. Either Li^{+} or F^{+} ions can desorb from the surface by the Coulomb repulsive force between a F^{+} ion and the first nearest Li^{+} ions. Since the residence time near the surface of Li^{+} ions is shorter than that of F^{+} ions, the difference in the spectra might be explained due to the re-neutralization probability of Li^{+} and F^{+} ions. However it is difficult to explain the structure of the F^{+} yield spectrum above 60 eV, since this probability should not depend on the photon energy.

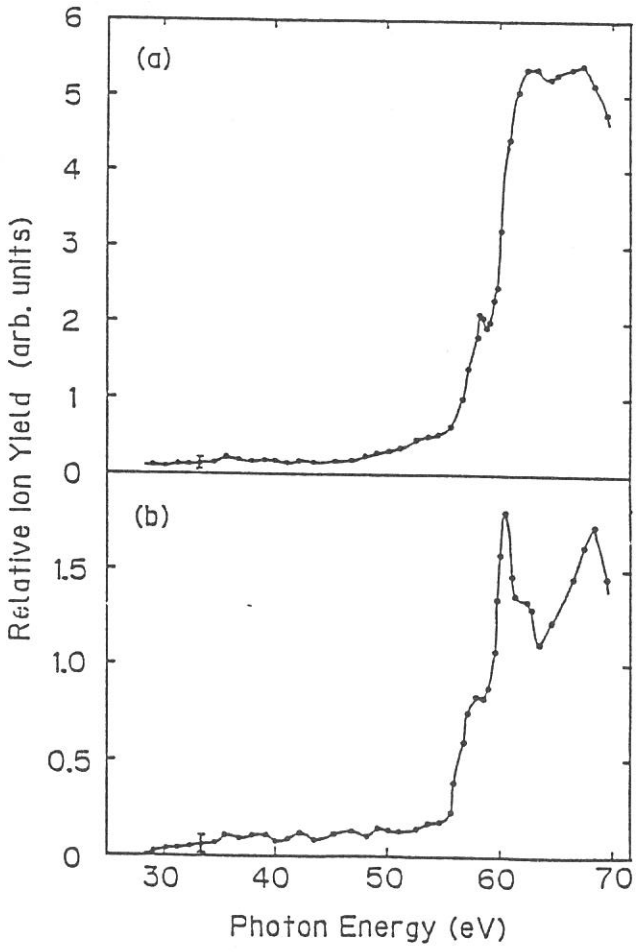

Fig. 1. Relative ion yield spectra. (a): Li^{+}, (b): F^{+}.

References

1) T.R. Pian et al., Surf. Sci. 128 (1983) 13.
2) C.C. Parks et al., Phys. Rev. B28 (1983) 4793.
3) C.C. Parks et al., Phys. Rev. B29 (1984) 4709.
4) B.F. Sonntag, Phys. Rev. B9 (1974) 3601.

FABRICATION OF X-RAY OPTICAL ELEMENTS BY SYNCHROTRON RADIATION X-RAY LITHOGRAPHY

Hiroaki ARITOME

Faculty of Engineering Science, Osaka University
Toyonaka, Osaka 560

I. Introduction

The advantage of synchrotron radiation as a source for x-ray lithography for LSI production is now well established. Synchrotron radiation x-ray lithography (abbreviated here as SR lithography) is a powerful tool also for fabricating x-ray optical elements such as transmission gratings and zone plates.

Elements of present interests are:

1) Transmission gratings for diagnostics of plasma of the laser nuclear fusion, space telescopes and synchrotron radiation spectroscopy.
2) Zone plates for diagnostics of plasma of the laser nuclear fusion, x-ray microscopes, synchrotron radiation spectroscopy and projection type x-ray lithography.

A pattern with a high aspect ratio (height/width) can be easily obtained by SR lithography even when the width is in the range of 20-100 nm. This is a very useful advantage from the point of application of synchrotron radiation to fabricate x-ray optical elements.

SR lithography is also applicable to fabricate the electronic devices of the next generation, the physical principles of which are different of those conventional. Conventionally, x-ray lithography means the proximity printing which is a way of pattern fabrication without optical lenses. This is due to the fact that it was difficult to get the x-ray lenses. In the case of fabricating patterns with 20-100 nm range, the projection type x-ray lithography with x-ray imaging elements should be preferable from the point of x-ray lithography as a mass production of future nanometer electronic devices. For this purpose, the optical system using layered synthetic materials (LSM) will be most promising. But, in special cases, zone plates can be also used. Those experiments are interesting because the spatial resolution of zone plates (20-50 nm) is better than the LSM according to the present technology.

From the above points, exposure characteristics of various x-ray resists such as PMMA (poly(methyl methacrylate)), FBM (poly(hexafluorobutyl methacrylate)), CMS (chloromethylated polystyrene) and CPMS (chloromethylated polymethylstylene) were investigated at the beam line BL-8A. The zone plates for synchrotron radiation spectroscopy of undulator radiation was succesfully fabricated by SR lithography and gold plating. The x-ray mask was fabricated by electron beam lithography and reactive ion ething or ion beam etching (1,2).

II) X-ray exposure experiments

The x-ray mask used was the free-standing zone plate with 250 zones, the focal length:200 mm (at the wavelength of 4.5 nm), a minimum zone width:0.97 um and 3 um thick gold. As a filter, 2 um-thick polyimide (Toray SP171) or 2 um-thick SiNx was used to cut off the long wavelength components. The energy of electrons in the ring was 600 MeV or 750 MeV. The energy of 600 MeV was mainly used. At the energy of 600 MeV, in the case of 2 um-thick SiNx, the wavelength range of 0.7-2.0 nm is effective for exposure and in the case of 2 um-thick polyimide the range of 0.7-2.7 and 4.5-8 nm is effective.

In the direct exposure of PMMA and CMS without a mask and a filter, the exposure time was 30 s for PMMA and 1 s for CMS at the beam current of 60 mA. This corresponds to the sensitivity of about 3000 mJ/cm^2 and 100 mJ/cm^2, respectively. Those values are close to the values reported.

For PMMA, the exposure time was 1 m for a 2 um-thick polyimide filter and 8 m for a 2 um-thick SiNx filter.

For FBM, the values were 30 s and 3 s, respectively. Those values are in reasonable agreement with calculated values assuming the absorption coefficient of the filter.

Figure 1 shows an example of the fabricated resit pattern of the above zone plate. From this resist pattern, the gold zone plate was succesfully fabricated by the gold plating. Those zone plates are especially useful for the linear monochromator for spectroscopy by the undulator radiation where the beam profile is nearly circular. The experiments of the linear monochromator is now under progress.

References

1) H.Aritome, H.Aoki, and S.Namba:J.Vac.Sci.Technol. B3 (1985) 265.
2) H.Aritome, K.Nagata, and S.Namba:in "Microcircuit Engineering 85" (K.D.van der Mast and S.Radelaar, Eds., North-Holland, 1985) p.459.

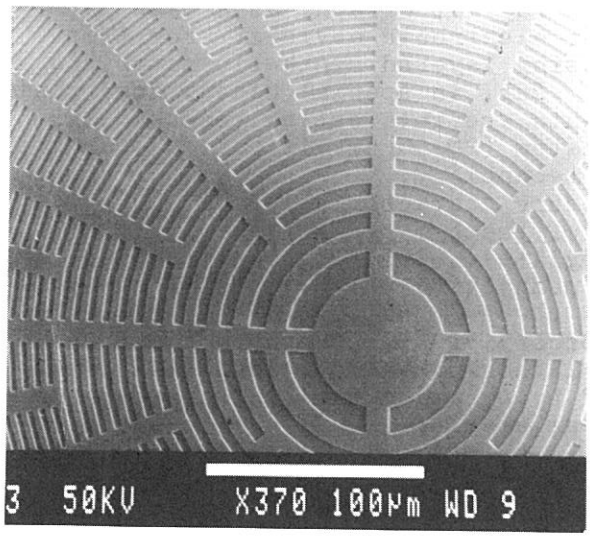

Fig. 1
PMMA resist pattern of a zone plate.

X-RAY VACUUM LITHOGRAPHY

Masaru HORI, Hitomi YAMADA, Takashi YONEDA*, Shinzo MORITA* and Shuzo HATTORI

Department of Electronics, Nagoya University, Chikusaku, Nagoya 464
*Department of Electrical Engineering, Meijo University, Tenpakuku, Nagoya 468

Synchrotron radiation (SR) was successfully applied to vacuum lithography with using plasma polymerizedd resist and plasma development, as shown in Fig. 1. Plasma polymerized methyl methacrylate (PPMMA) and the plasma copolymerized methyl methacrylate with tetramethyltin (TMT), SF_6, I_2 or styrene were prepared by using an inductively coupled gas flow type reactor. The polymer structures of these resists were investigasted by ESCA. ESCA results showed that a small amount of S, F, Sn and I were incorporated into the polymer matrix.

The plasma polymerized resists were exposed to SR under the conditions of 600 MeV and a current of 30 mA directly or through an X-ray mask made of polyimide menbrane and Ta absorbent in a vacuum chamber. SR irradiated resists showed the self development phenomenon. The self developed resists depth by SR exposure without the mask was measured as a function of exposure duration. The results are shown in Fig. 2. It was found that the removed thickness of all resists increased linearly with increasing dose in the low doses region, while it was saturated completely at the high doses region. The self development was enhanced significantly by doping Sn, S and I. In order to confirm the fine pattern fabrication by this method, duplication of mask pattern was examined on the PP(MMA+TMT) resist. The mask pattern of linres and spaces with 1 um width was replicated faithfully on the resists.

The hollowed patterns by self developmenbt were served to O_2 plasma etching in the apparatus with parallel plate electrodes at a gas pressure of 0.5 Pa and a discharged power of 50 W. The results of plasma etching on PPMMA exposed to SR is shown in Fig. 3. The enhancement of differential thickness was observed on the film exposed for 10 min that the self development characteristic altered from increasing to saturating at the duration in Fig. 2. However, the differential thickness decreased with increasing etching duration on exposed 30 min, that the self development was completely saturated at the duration as shown in Fig. 2.

In order to investigate the reaction mechanism of above mentioned self development and plasma development characteristics, IR and ESCA were performed on the same film before and after SR exposure. Also the gas fragments generated from the resists during SR exposure were detected by mass spectroscopy.

From these analyses , it was concluded that PPMMA and its plasma copolymerized resists undergo the elimination of ester structure as the primary degrading reaction by SR exposure and at high doses, the recombination of the dissociated groups have been proceeding, resulting in resist carbonization involving C=C bond,

which was hard enough to withstand the furthermore SR exposure and also retarded the etching rate for oxygen plasma.

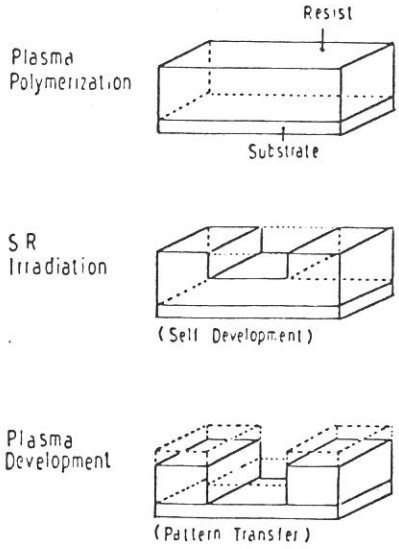

Fig. 1 Process steps

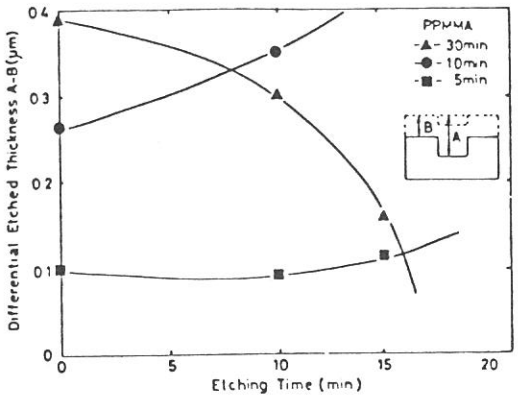

Fig. 3 Plasma etching characteristic in PPMMA.

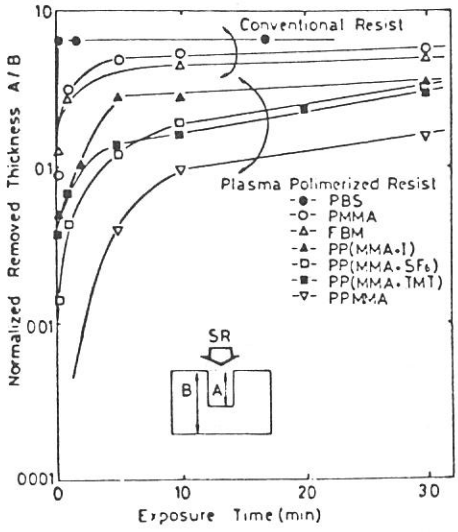

Fig. 2 Self development characteristics.

X-RAY TOPOGRAPHIC STUDY OF *p*-CHLOROBENZAMIDE SINGLE CRYSTAL

Masahiro MORI, Tokuo MATSUKAWA, Masayoshi OBASHI, Takatoshi MURATA*, Shun-ichi NAOE** and Yasuo NISHIHATA***

College of General Education, Osaka University, Toyonaka, Osaka 560
*Kyoto University of Education, Kyoto 612
**College of Liberal Arts, Kanazawa University, Kanazawa, Ishikawa 920
***Department of Physics, Kwansei-Gakuin University, Nishinomiya, Hyogo 662

Introduction

Synchrotron radiation light source has very good directionality. Recently, x-ray topography technique develops rapidly using this character of the synchrotron radiation. It is interesting to apply this technique to the phase transition phenomena (reference 1). It is probable that superlattice reflections are more influenced by the phase transition than the main Bragg reflections, as they only appear under the transition temperature. Our aim is the study of the difference between both refrections.

This experiment is the first step of this aim. At first, we have to take into consideration that the shortest wavelength is 9Å when UVSOR operates at 600MeV and 100mA.

Experimental

Triclinic *p*-chlorobenzamide was chosen for the sample. The transition temperature of this sample is about 40°C. Crystal data are a=15.027, b=5.481, c=14.486, α=97.84, β=111.99, and γ=95.17 from reference 2. Crystals obtained from an ethanol solution had a shape elongated along b axis. The typical size of these samples is about 10x40x3 mm^3. It has previously been ascertained that they are triclinic structures with photographic methods. The other main aim of this time experiment is the estimation of the practical intensitiy of UVSOR.

We took the diffraction photographs putting white synchrotron radiation beam on the single crystal with Back Laue Photographic method. X-ray films were covered with 15μm-thick aluminium foil to be prevented from visible light. The experiment was done as follow conditions:

synchrotron energy	600MeV
synchrotron current	80mA
exposed time	6.0minutes
observed diffraction angles	from 110° to 172°
slit	full open
temperature	room temperature

Results and discussions

Superlattice reflections could not be ascertained as these intensities are not strong. Four Bragg spots were observed on x-ray films. The figure is the picture of one of them at about 168 diffraction angles. The outlook of defects is reflected in such a kind of photograph. But this figure is too complicated to understand it. It is seemed that this shows the behavior

of crystal growth in an ethanol solution. Further discussions can not be done to see it of such complicated materials. It is necessary to do such a kind of experiment to choose and use more simple crystals. It is more important to use shorter wavelength x-ray source. In the case that synchrotron operates at 750 MeV, the shortest wavelength is 5Å. When the wiggler apparatus operates, it is only 2Å.

References

1) S. Suzuki, H.Kawata and M. Ando ; Photon Factory Activity Report 1983/84 page VI-135
2) T. Taniguchi, K. Nakata, Y. Takaki and K. Sakurai ; Acta Cryst. B34 (1978) 2574